

Comparison of heuristics and metaheuristics for topology optimisation in acoustic porous materials

Vivek T. Ramamoorthy,^{1, a)} Ender Özcan,¹ Andrew J. Parkes,¹ Abhilash Sreekumar,² Luc Jaouen,³ and François-Xavier Bécot³

¹*Computational Optimisation and Learning Lab, School of Computer Science, University of Nottingham, NG8 1BB, United Kingdom*

²*Centre for Structural Engineering and Informatics, Faculty of Engineering, University of Nottingham, NG7 2RD, United Kingdom*

³*Matelys-Research Lab, 7 Rue des Maraîchers, Vaulx-en-Velin, 69120, France*

(Dated: 27 October 2021)

When designing sound packages, often fully filling the available space with acoustic materials is not the most absorbing solution. Better solutions can be obtained by creating cavities of air pockets, but determining the most optimal shape and topology that maximises sound absorption is a computationally challenging task. Many recent topology optimisation applications in acoustics use heuristic methods such as solid-isotropic-material-with-penalisation (SIMP) to quickly find near-optimal solutions. This study investigates seven heuristic and metaheuristic optimisation approaches including SIMP applied to topology optimisation of acoustic porous materials for absorption maximisation. The approaches tested are hill climbing, constructive heuristics, SIMP, genetic algorithm, tabu search, covariance-matrix-adaptation evolution strategy (CMA-ES), and differential evolution. All the algorithms are tested on seven benchmark problems varying in material properties, target frequencies, and dimensions. The empirical results show that hill climbing, constructive heuristics, and a discrete variant of CMA-ES outperform the other algorithms in terms of the average quality of solutions over the different problem instances. Though gradient-based SIMP algorithms converge to local optima in some problem instances, they are computationally more efficient. One of the general lessons is that different strategies explore different regions of the search space producing unique sets of solutions.

©2021 Acoustical Society of America. [<http://dx.doi.org/DOI number>]

[XYZ]

Pages: 1–14

1 I. INTRODUCTION

2 A. Background

3 Historically, shape designs in engineering have been
4 arrived at via a trial-and-error process, intuition, incre-
5 mental improvements to old designs, human decision-
6 making from numerical analyses, and recently, solely by
7 computer analyses. Superior-to-human engineering de-
8 signs have been achieved by computers using technolo-
9 gies such as structural topology optimisation. Topology
10 optimisation involves finding the optimal topology (num-
11 ber of holes) and shape (size, dimensions) for a structure
12 such that a given performance indicator is either max-
13 imised or minimised. Bendsøe and Kikuchi¹ introduced
14 the concept of simultaneously optimising both shape and
15 topology in the late 1980s. Since then, many theoretical
16 developments have been made, and a community of re-
17 searchers have actively been working in this field. One of
18 the ways to formulate a topology optimisation problem is
19 finding the optimal assignment of materials in each finite

20 element of a discretised structure. In principle, this for-
21 mulation is discrete optimisation, and finding the exact
22 global optimum is computationally challenging. Exact
23 optimisation techniques that guarantee finding the global
24 optimum remain prohibitively expensive. Evaluating all
25 possible solutions becomes impractical due to the large
26 search space sizes and the expensive finite element eval-
27 uations. A noteworthy effort towards topology optimisa-
28 tion using an exact approach was by Stolpe and Bendsøe²
29 on the Zhou and Rozvany problem instance³. But justifi-
30 ably, the focus of previous work has mainly been on the
31 inexact or *heuristic* optimisation approaches.

32 B. Heuristics

33 Heuristics are techniques that find solutions close
34 enough to the global optimum in a reasonable time.
35 Though heuristics do not guarantee finding the optimal
36 solution, they are well-established and often the only
37 viable option to address hard problems, such as those
38 in NP-complete and NP-hard classes. The three most
39 popular heuristic approaches applied to topology optimi-
40 sation problems are SIMP^{1,4-6} (solid-isotropic-material-

^{a)} vivek.thaminniramamoorthy@nottingham.ac.uk

with-penalisation), BESO⁷⁻⁹ (bi-directional evolutionary structural optimisation), and the level-set method¹⁰⁻¹². Among these, SIMP is the most commonly used and well-studied approach. In SIMP, the discrete material assignment problem is relaxed to the continuous space by allowing intermediate materials between solid and void. A penalty-based material interpolation scheme is used to represent intermediate materials and gradient-based optimisation strategies such as optimality criteria¹³ or method of moving asymptotes¹⁴ is used to move across the design variable space to find a near-optimal design. As SIMP is a derivative-based technique, it requires that a sensitivity analysis be carried out. BESO, not to be confused with evolutionary algorithms despite its name, is a type of constructive approach which iteratively adds material where stresses are high and removes material where stresses are low to arrive at a design. In the level-set method, a scalar field is associated with the design domain region and the isosurfaces of this scalar field are made the boundaries of the topology. This scalar field is then optimised to optimise the topology.

C. Metaheuristics

While heuristics are quick strategies to find near-optimal solutions, it was realised by Glover¹⁵ that many powerful heuristic approaches follow certain higher-level guidelines. These guidelines can be considered heuristics to design heuristic algorithms, and hence are termed *metaheuristics*. A popular example of a metaheuristic is genetic algorithms, wherein the guideline is to initiate a population of solutions, apply selection pressure to pick good individuals, recombine the selected individuals, mutate them and replace them into the population. Numerous metaheuristic techniques, such as genetic algorithms and CMA-ES, have also been studied on structural topology optimisation problems^{16,17}.

D. Acoustic topology optimisation

Theoretical developments in structural topology optimisation have focused on the classical problem of compliance minimisation^{18,19}. Nevertheless, the application of topology optimisation techniques to other problem domains is steadily on the rise^{18,20,21}. These techniques have already been extended to acoustics, giving rise to a sub-field called acoustic topology optimisation.

At the time of writing this article, topology optimisation has been performed on a variety of acoustic applications, including horns, mufflers, rooms and sound barriers²²⁻³⁶. A majority of these applications use the gradient-based SIMP method or its variants, while a small fraction of them use BESO or level-set methods. These applications can be categorised into acoustic fluid-structure interaction problems and porous material problems. In acoustic fluid-structure interaction problems, the material choices are non-porous solid and fluid phases, and the wave propagation is modelled using mixed formulations^{37,38}. Within acoustic

fluid-structure interaction, problems other than topology optimisation such as material parameter estimation³⁹ have also found the application of gradient-based methods such as the method of moving asymptotes⁴⁰. In porous material topology optimisation problems, the material choices also include poroelastic materials, and specialised Biot formulations^{41,42} are generally used. In some applications^{31,43}, boundary element method is used to optimise the boundary topology instead of the bulk topology. In this article, poroelastic material topology optimisation is in focus. Specifically, we refer to topology optimisation in the context of finding optimal mesoscale shapes and topologies, i.e., in the order of magnitude of the material thickness, and not the optimisation of their microstructures.

Although metaheuristics have been previously tested on classical structural topology optimisation problems^{16,17}, their use has been limited in acoustic topology optimisation applications^{44?}. Only a few optimisation approaches have been tested, and optimisation theory exclusive to this problem domain remains yet to be explored. The present work is a step in this direction.

E. Contributions in this work

The goal of the present work is to investigate the performance of alternative heuristic optimisation approaches, including a few well-known metaheuristic approaches on a set of benchmark problems. In this article, the approaches compared are hill climbing, constructive heuristics, SIMP, genetic algorithms, tabu search, CMA-ES and differential evolution. While SIMP and its variants use gradients, none of the other approaches use any domain-specific information from the problem other than the objective function. Optimisation tests show how different approaches perform for various CPU time budgets. Notably, while SIMP algorithms produce good-quality solutions at low CPU time budgets, certain other algorithms such as hill climbing, constructive heuristics and CMA-ES outperform at higher computational budgets. The findings reported in this paper may serve as a useful prelude to develop better strategies for topology optimisation in acoustic porous materials.

The article is organised as follows: the optimisation problem description and the modelling methodology are given in section II, concise descriptions and settings of the optimisation approaches are given in section III, the results from the optimisation tests are discussed in section IV, and the conclusive remarks are provided in section V. Further, the pseudocodes of all algorithms, runtime comparisons, solution quality distributions and final optimal shapes from all algorithms for all problem instances are included in the supplementary material.

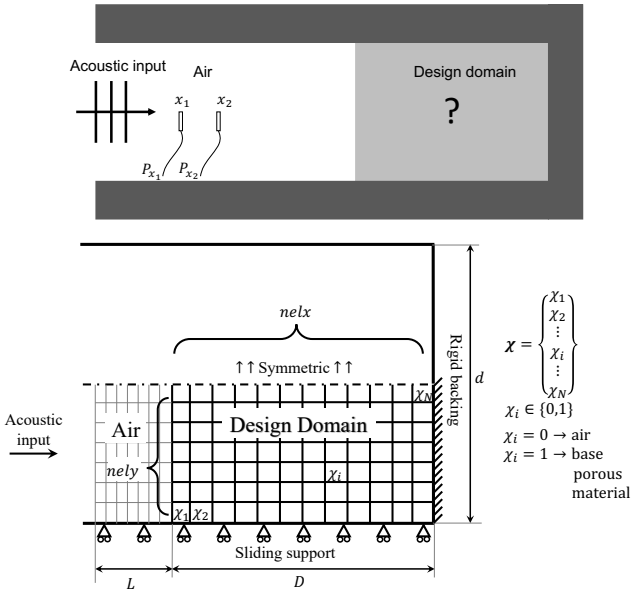


FIG. 1. Finite element model of an impedance tube system with the design domain where the shape and topology of a poroelastic material is to be optimised.

147 II. PROBLEM DESCRIPTION AND MODELLING

148 A. Maximising sound absorption in normal incidence

149 Consider the following problem: Given a finite ele-
 150 ment model of an impedance tube as shown in Figure 1,
 151 what is the best assignment of either air or a given poro-
 152 elastic material to each element in the design domain that
 153 maximises the sound absorption of an acoustic source.
 154 The optimisation formulation can be written as:

$$\max_{\chi_i} \bar{\alpha}(\chi) = \frac{1}{n} \sum_{f=f_1}^{f_n} \alpha(\chi, f) \quad (1)$$

$$\chi : \chi_i \in \{0, 1\} \quad \forall \quad i = 1, 2, \dots, N$$

$$\bar{\alpha} \in [0, 1]$$

where $\alpha(\chi, f)$ is the sound absorption coefficient in normal incidence for a given shape χ for frequency f , χ_i are the decision variables represent the choice between air and porous material for the i^{th} element, N is the number of elements in the design domain, and f_1, f_2, \dots, f_n are the target frequencies for which the mean absorption is to be maximised (where n is the number of frequencies considered). The symbol $\bar{\alpha}$ is used to refer to the mean sound absorption coefficient (α) across the target frequencies. In this paper, $\bar{\alpha}$ may be referred to as simply *absorption* or *fitness*, which is to be maximised. Note that in the problem formulation 1, a volume fraction constraint is not included, which is unlike in usual topology optimisation problems. One reason is that in porous material topology optimisation, often the optimal shapes need to be

carved out from a large block of the base porous material. The removed material may not often constitute material-saving, as the cost of recycling the carved out material could negate the material-saving benefit. Another reason is that more optimisation approaches to be tested as the formulation would resemble a conventional discrete optimisation problem. Without the volume constraint, since two choices are available (air or the base porous material) for each of the N elements in the design domain the search space size becomes 2^N . If a limit V_f is imposed on the ratio of porous volume to the total volume in the design domain ($\frac{1}{N} \sum_{i=1}^N \chi_i = V_f$), the search space size would become ${}^N C_{(V_f N)}$. In both these cases, the number of feasible solutions grows quickly with an increase in N . Since discrete optimisation is considered difficult to solve, the problem is usually relaxed to a continuous problem allowing χ_i to take values between 0 and 1, in other words allowing intermediate materials between air and porous material in the design domain. The problem is then solved using continuous optimisation approaches. Intermediate materials given by $\chi_i \in (0, 1)$ are modelled using interpolating the material properties. One such interpolation scheme is the SIMP scheme (not to be confused with the SIMP approach). Using this scheme, the material property ψ for the intermediate material is given by equation 2.

$$\psi_i = \psi_{air} + \chi_i^p [\psi_{por} - \psi_{air}] \quad (2)$$

$$\psi \in \{E, \nu, \tilde{\rho}, \tilde{\gamma}_s, \tilde{\rho}_{eq}, \tilde{\mathbf{K}}_{eq}\} \quad (3)$$

155 Here, ψ is any material property from Young's modulus (E), Poisson's ratio (ν), modified Biot density ($\tilde{\rho}$),
 156 coupling factor ($\tilde{\gamma}_s$), dynamic mass density ($\tilde{\rho}_{eq}$), dy-
 157 namic bulk modulus ($\tilde{\mathbf{K}}_{eq}$) etc. Though filtering tech-
 158 niques and interpolation penalties are used to enforce
 159 discrete solutions in such continuous formulations, often
 160 the resulting solutions tend to have intermediate mate-
 161 rials i.e. $\chi_i \in (0, 1)$. Since filters in topology opti-
 162 mation play a role in the optimisation performance, in
 163 this study no filters or manufacturability restrictions are
 164 considered —with the view that these can be done in
 165 post-processing.

167 B. Computing sound absorption and its gradients

168 To compute sound absorption, the poroelastic system
 169 constituting the fixed and design domains is modelled
 170 using the alternative Biot finite element formulations de-
 171 scribed by Bécot and Jaouen⁴². This formulation is based
 172 on the mixed $\{\mathbf{u}, \mathbf{P}\}$ formulation by Atalla *et al.*⁴¹. The
 173 acoustic model for the fluid part is given by the Johnson-
 174 Champoux-Allard-Lafarge (JCAL)^{45–47} model. To nat-
 175 urally account for the interface between porous and air
 176 regions, the unified analysis approach proposed and ver-
 177 ified by Lee *et al.*²⁴ is adopted. For intermediate material
 178 properties between air and porous material, the SIMP
 179 interpolation scheme⁴⁸ is used. The poroelastic system
 180 governing equations can be expressed in matrix form in

181 equation 4.

$$\underbrace{\begin{bmatrix} \tilde{\mathbf{K}} - \omega^2 \tilde{\mathbf{M}} & -\tilde{\mathbf{C}} \\ -\tilde{\mathbf{C}}^T & \tilde{\mathbf{H}}/\omega^2 - \tilde{\mathbf{Q}} \end{bmatrix}}_{\tilde{\mathbf{S}}(\omega)} \underbrace{\begin{Bmatrix} \{\mathbf{u}\} \\ \{\mathbf{P}\} \end{Bmatrix}}_{\tilde{\mathbf{X}}(\omega)} = \underbrace{\begin{Bmatrix} \tilde{\mathbf{F}}_u \\ \tilde{\mathbf{F}}_P/\omega^2 \end{Bmatrix}}_{\tilde{\mathbf{F}}} \quad (4)$$

182 where $(\tilde{\cdot})$ denotes the complex-valued nature of it's argu-
 183 ment. The expressions for the state matrices $\tilde{\mathbf{K}}$, $\tilde{\mathbf{M}}$, $\tilde{\mathbf{H}}$,
 184 $\tilde{\mathbf{Q}}$ and $\tilde{\mathbf{C}}$ are functions of the topological design/decision
 185 variables $\boldsymbol{\chi}$. The construction of these matrices are ex-
 186 plained by Atalla *et al.*⁴¹ and will not be detailed here.
 187 $\{\mathbf{u}\}$ and $\{\mathbf{P}\}$ denote the solid phase displacement and
 188 fluid phase pressure degrees of freedom in the poroelastic
 189 system respectively. The associated global stiffness ma-
 190 trix $\tilde{\mathbf{S}}(\omega)$ and the load vector $\tilde{\mathbf{F}}$ are iteratively assembled
 191 over each angular frequency $\omega = 2\pi f$ to yield a system of
 192 linear equations. These equations are solved as given in
 193 equation 5 to obtain the solution vector $\tilde{\mathbf{X}}(\boldsymbol{\chi}, \omega)$ which
 194 will contain the displacement and pressure fields of the
 195 solid and fluid parts of the poroelastic material respec-
 196 tively.

$$\{\tilde{\mathbf{X}}(\boldsymbol{\chi}, \omega)\} = [\tilde{\mathbf{S}}(\boldsymbol{\chi}, \omega)]^{-1} \{\tilde{\mathbf{F}}\} \quad (5)$$

197 For normal incidence, assuming plane waves, the sound
 198 absorption coefficient can be computed using the two-
 199 microphone method. Considering two closely spaced
 200 points x_1 and x_2 in the air region, the complex pres-
 201 sure amplitudes in frequency domain P_{x_1} and P_{x_2} can
 202 be obtained from $\{\mathbf{P}\}$ in $\tilde{\mathbf{X}}$. The plane wave reflection
 203 coefficient \tilde{R}_c can then be computed from these pressures
 204 as,

$$\tilde{R}_c(\boldsymbol{\chi}, \omega) = \frac{P_{x_1}(\boldsymbol{\chi}, \omega)e^{-ikx_2} - P_{x_2}(\boldsymbol{\chi}, \omega)e^{-ikx_1}}{-P_{x_1}(\boldsymbol{\chi}, \omega)e^{ikx_2} + P_{x_2}(\boldsymbol{\chi}, \omega)e^{ikx_1}} \quad (6)$$

205 Here, k is the wave number given by ω/c_{air} with c_{air}
 206 being the speed of sound in air. The sound absorption
 207 coefficient α is then given by:

$$\alpha(\boldsymbol{\chi}, \omega) = 1 - |\tilde{R}_c(\boldsymbol{\chi}, \omega)|^2 \quad (7)$$

208 The analytical gradient of absorption can be com-
 209 puted by using chain rule following a similar procedure
 210 to that of Lee *et al.*²⁴. From equation 7:

$$\frac{\partial \alpha}{\partial \chi_i} = -2|\tilde{R}_c| \frac{\partial |\tilde{R}_c|}{\partial \chi_i} \quad (8)$$

211

$$\frac{\partial |\tilde{R}_c|}{\partial \chi_i} = \frac{\Re(\tilde{R}_c \times \overline{\frac{\partial \tilde{R}_c}{\partial \chi_i}})}{|\tilde{R}_c|} \quad (9)$$

212 Equation 9 computes the derivative of absolute of
 213 the complex-valued \tilde{R}_c , $\Re(\cdot)$ is the real part and (\cdot) is
 214 the complex conjugate operator. The gradient $\frac{\partial \tilde{R}_c}{\partial \chi_i}$ is
 215 obtained from $\frac{\partial P_{x_1}}{\partial \chi_i}$ and $\frac{\partial P_{x_2}}{\partial \chi_i}$, which in-turn are two ele-

216 ments from the derivative vector $\frac{\partial \tilde{\mathbf{X}}}{\partial \chi_i}$. To find $\frac{\partial \tilde{\mathbf{X}}}{\partial \chi_i}$, equa-
 217 tion 5 is differentiated to get the following expression.

$$\frac{\partial}{\partial \chi_i} \tilde{\mathbf{X}}(\boldsymbol{\chi}, \omega) = [\tilde{\mathbf{S}}(\omega)]^{-1} \frac{-\partial[\tilde{\mathbf{S}}(\omega)]}{\partial \chi_i} \tilde{\mathbf{X}} \quad (10)$$

The above step involves a large matrix inversion followed
 by sparse matrix and vector multiplications repeated for
 each element in the design domain. This step is per-
 formed efficiently by using the adjoint-based approach as
 detailed by Lee, Göransson and Kim²⁸. Since only two
 elements in $\frac{\partial \tilde{\mathbf{X}}}{\partial \chi_i}$ i.e. $\frac{\partial P_{x_1}}{\partial \chi_i}$ and $\frac{\partial P_{x_2}}{\partial \chi_i}$ need to be computed
 to compute the gradients, one can premultiply the equa-
 tion 10 by the term $\frac{\partial P_{x_1}}{\partial \chi_i}$, which is a vector of 0s except
 for one element with a value of 1 corresponding to the
 P_{x_1} degree of freedom in equation 10.

$$\begin{aligned} \frac{\partial P_{x_1}}{\partial \chi_i} &= \left(\frac{\partial P_{x_1}}{\partial \mathbf{X}} \right)^T \frac{\partial \tilde{\mathbf{X}}}{\partial \chi_i} \\ &= \left(\frac{\partial P_{x_1}}{\partial \mathbf{X}} \right)^T [\tilde{\mathbf{S}}]^{-1} \frac{-\partial[\tilde{\mathbf{S}}]}{\partial \chi_i} \tilde{\mathbf{X}} = \lambda_{x_1}^T \frac{-\partial[\tilde{\mathbf{S}}]}{\partial \chi_i} \tilde{\mathbf{X}} \end{aligned} \quad (11)$$

218 Then, one can find a fictitious response vector $\lambda_{x_1} =$
 219 $[\tilde{\mathbf{S}}]^{-1} \frac{\partial P_{x_1}}{\partial \mathbf{X}}$ and compute $\frac{\partial P_{x_1}}{\partial \chi_i}$ for each i by computing
 220 $\lambda_{x_1}^T \left(\frac{-\partial[\tilde{\mathbf{S}}]}{\partial \chi_i} \tilde{\mathbf{X}} \right)$ quickly. This avoids solving system of equa-
 221 tions repeatedly for each element or performing explicit
 222 matrix inversions. The above step is crucial for speeding-
 223 up gradient methods. In addition to solving $[\tilde{\mathbf{S}}(\omega)]^{-1} \tilde{\mathbf{F}}$,
 224 two additional instances of solving system of equations is
 225 involved in finding λ_{x_1} and λ_{x_2} . Assuming all other steps
 226 are time insignificant, function evaluation with gradients
 227 are approximately three times as expensive as evaluating
 228 without gradient.

229 This procedure has to be repeated at each frequency
 230 ω and for fine frequency steps, the calculation could be-
 231 come expensive. Although not implemented in this work,
 232 it is worth noting that there exist various expansion
 233 methods^{???} to speed up the computation for broad
 234 frequency range problems.

235 Further, the gradients $\frac{-\partial[\tilde{\mathbf{S}}]}{\partial \chi_i}$ are obtained by
 236 applying chain rule up to the material properties
 237 $(E, \nu, \tilde{\rho}, \tilde{\gamma}_s, \tilde{\rho}_{eq}, \tilde{\mathbf{K}}_{eq})$ which depend on the design vari-
 238 ables $\boldsymbol{\chi}$.

239 C. Benchmark problem instances

240 For comparing the performance of various optimi-
 241 sation approaches, seven benchmark problem instances
 242 with different characteristics as given in Table I are
 243 utilised. A two-dimensional finite element model of a
 244 small rectangular unit cell of an absorbing wall, as shown
 245 in Figure 1 is considered. The unit cell's dimensions, its
 246 discretisation into finite elements, the base porous ma-
 247 terial to fill the elements, and target frequencies to be
 248 absorbed vary for each problem instance.

249 The unit cell of height d is backed by a rigid wall on
 250 the right, and a normal incidence sound source is mod-

TABLE I. Benchmark problem instances (see section II C)

No.	Problem instance name	Mesh size nelx × nely	Length D (m)	Height d (m)	f_{min} Hz	f_{step} Hz	f_{max} Hz	Material ID (see Table II)
1	LKKK material broadband coarse-mesh	10 × 10	0.135	0.054	100	100	1500	1
2	Melamine - building problem	15 × 10	0.045	0.1	100	100	1500	2
3	High resistivity foam - low frequency	10 × 10	0.1	0.1	50	50	500	3
4	Melamine - automotive problem	10 × 10	0.02	0.1	100	100	1500	2
5	Melamine - high frequency problem	10 × 10	0.02	0.1	2000	1000	5000	2
6	Melamine -broadband fine-mesh	50 × 20	0.135	0.054	100	100	1500	2
7	Melamine -single target frequency	10 × 5	0.135	0.054	500	500	500	2

TABLE II. Acoustic and elastic properties of materials used in the benchmark problems in Table I. Here, ϕ is the open porosity, Λ' is the thermal characteristic length, Λ is the viscous characteristic length, σ is the static airflow resistivity, α_∞ is the tortuosity, k'_0 is the thermal permeability, ρ is the bulk density, E is the solid elastic modulus, ν is the Poisson's ratio and η is the dissipation factor.

Material parameters	Material-1	Material-2	Material-3
Material:	LKKK ²⁴	Melamine	High-resistivity soft foam
Acoustic model:	JCAL	JCAL	JCAL ⁴⁵⁻⁴⁷
ϕ	0.9	0.99	0.8
Λ' (μm)	449	196	100
Λ (μm)	225	98	10
σ ($\text{N}\cdot\text{s}\cdot\text{m}^{-4}$)	25000	10000	300000
α_∞	7.8	1.01	3
k'_0	4.75e-09	4.75e-09	4.75e-09
ρ ($\text{kg}\cdot\text{m}^{-3}$)	31.08	8	80
E (Pa)	800000	160000	30000
ν	0.4	0.44	0.44
η	0.265	0.1	0.01

elled at the left end. A region from the rigid wall up to a length D is designated as the design domain. The design domain is followed by a fixed domain, which is just an air region in this case with a length L . The design domain is discretised into $nelx$ and $nely$ finite elements along the horizontal and vertical directions respectively. Within the unit cell, symmetry is assumed about the central horizontal line, and sliding boundaries (u_x -free, $u_y = 0$, P -free) are assumed at the top and bottom edges. To save computational effort, only half of the system is modelled, and symmetry is imposed about the centerline (u_x -free, $u_y = 0$, P -free). It has been verified that this gives the same absorptions as obtained when modelling the full unit cell with sliding supports in the top and bottom edges. In all the problem instances, the mean sound

absorption coefficient under normal incidence across the target frequencies is to be maximised.

Although meant to be arbitrary, the problem instances are chosen from practical engineering examples. The material used for optimisation for each problem instance is picked from three choices in Table II. In problem instance 1, a special material previously used by Lee, Kim, Kim, and Kang²⁴ (LKKK material) is used on a coarser 10×10 discretisation. Note that the LKKK material may not be representative of a physical material due to the high tortuosity value of 7.8. Problem instance 2 features a 45 mm long design domain representative of a typical building application. Problem instance 3 uses an artificial material with a high static airflow resistivity. In problem instance 4, a thin design domain of 2 cm, representative of a foam layer in an automotive absorber, is considered. In problem instance 5, a thin layer is optimised for high-frequency absorption. Among the problem instances, problem instance 6 has a relatively fine mesh size with 50×20 elements featuring a thicker design domain optimised on a broad frequency range. Other than 1 and 3, all problem instances use Melamine foam for control. In problem instance 7, a single target frequency is considered.

III. OPTIMISATION APPROACHES

Several gradient-free heuristic and metaheuristic approaches, including well known and novel, are evaluated in this study alongside the state-of-the-art gradient-based approach SIMP. Henceforth in this paper, all the heuristic and metaheuristic approaches will be referred to as *algorithms*, and they are not to be confused with *exact* algorithms as used by some authors. The algorithms tested and their settings are summarised in Table III.

Five heuristic algorithms namely HC, CH1, CH2, SIMPf0 and SIMPf2 are tested. HC is a first-improvement hill climbing, where each element is flipped between air and porous material, and the new solution is accepted if it is improving. Consecutive elements are flipped like in a raster scan (row-by-row) until the function evaluation budget is used up. CH1 is a constructive heuristic that starts from an air-filled solution and progressively adds porous material in elements of best improvement in absorption. Similarly, CH2 starts from a

TABLE III. Optimisation approaches tested (pseudocodes are included in the supplementary material)

Abbr.	Optimisation approach	Procedure and parameter settings	Algorithm type: Deterministic or Non-deterministic	Trials	Search space	Gradient usage	Fn. eval. budget
HEURISTICS							
HC	Hill climbing (first improvement)	Start with a random binary array solution; Bit flip the consecutive elements; Accept if improving and move to the next element; Repeat from the start unless fn. eval. budget is used up. Element ordering is like in a raster scan.	Non-deterministic since starting solution is random	31	Discrete	No	4096
CH1	Constructive heuristic: material addition	Start with air-filled design domain; Compute absorption improvement at each element by filling porous material only in that element; Sort elements; Add porous material at best 'm' improving elements; Repeat until design domain is fully porous; Track and return the best solution. m is chosen such that the budget is not exceeded.	Deterministic	1	Discrete	No	4096
CH2	Constructive heuristic: material removal	Similar to CH1. Start from fully porous design domain; Remove porous (replace with air) at 'm' least worsening elements; Repeat until all porous is removed; Track and return the best solution	Deterministic	1	Discrete	No	4096
SIMPf0	SIMP with no filter ⁴⁹	Start from a random continuous solution, follow the SIMP procedure ⁴⁹ ; Omit the filtering step. Use SIMP penalty $p = 3$; move update - optimality criteria; move limit $m = 0.2$; Volume fraction limit $V_f = 1$.	Non-deterministic	31	Continuous	Yes	1366
SIMPf2	SIMP with density filter ⁴⁹	Start from a random continuous solution, follow the SIMP procedure ⁴⁹ ; use density filter $ft=2$. Use SIMP penalty $p = 3$; move update - optimality criteria; move limit $m = 0.2$; Volume fraction limit $V_f = 1$; Filter radius $r_{min} = 2$.	Non-deterministic	31	Continuous	Yes	1366
METAHEURISTICS							
GA	Genetic algorithm ⁵⁰	Initialise population with 64 random binary solutions; Selection: tournament-2; Crossover: uniform; Mutation: bitflip; Mutation rate: $1/(N)$; Replacement: best of parents and offspring replace parents; Repeat from selection, unless budget is used up.	Non-deterministic (uses a random number generator)	31	Discrete	No	4096
TABU	Tabu search ⁵¹	Initiate tabu list; Start with a random binary array solution; Pick a random bit, not in tabu list; Accept if improving and add the bit to tabu list; tabu tenure: 20% of N ; Pick another random bit and repeat unless budget is used up.	Non-deterministic (since starting solution and moves are random)	31	Discrete	No	4096
CMA	Covariance-matrix-adaptation evolution strategy ⁵²	Relax problem to continuous using SIMP interpolation scheme with $p = 3$; Follow CMA procedure ⁵² ; Terminate if budget is used up; Discretise final continuous solution by rounding.	Non-deterministic (uses a random number generator to sample points from the distribution)	31	Continuous	No	4096
CMAAd	Discrete variant of CMA	Follow CMA procedure in continuous space; Before fitness evaluation, discretise the sampled continuous solutions by rounding; Return the rounded best solution. An interpolation scheme is not necessary as continuous solutions are never evaluated.	Non-deterministic	31	Discrete	No	4096
DE	Differential evolution ^{53,54}	Relax problem to continuous using SIMP interpolation scheme with $p = 3$; Follow differential evolution procedure ^{53,54} ; Stop if budget is used up. Use population size=32; F=0.2; CR=0.2;	Non-deterministic	31	Continuous	No	4096
DEd	Discrete variant of DE	Follow the differential evolution procedure; Before fitness evaluation, discretise the sampled continuous solutions by rounding; Return the rounded best solution.	Non-deterministic	31	Discrete	No	4096

309 porous material-filled solution and progressively removes 314 step. While SIMPf2 uses density filtering, SIMPf0 uses
 310 porous material from the elements where the decrease in 315 no filtering techniques.
 311 absorption is the least. SIMPf0 and SIMPf2 are solid- 316 Four popular metaheuristic approaches are tested,
 312 isotropic-material-with-penalisation approaches⁴⁹ which 317 including genetic algorithm (GA), tabu search (TABU),
 313 use gradients of absorption to modify the solution at each 318 covariance-matrix-adaptation evolution strategy (CMA)

319 and differential evolution (DE). Additionally, discrete
320 variants of CMA and DE referred to as CMA_d and DE_d
321 are also tested, where the continuous shapes are rounded
322 before every absorption evaluation.

323 Except for CH1 and CH2, all the other algorithms
324 are non-deterministic as they embed a random compo-
325 nent, and each new trial of the non-deterministic algo-
326 rithm could produce a different near-optimal solution.
327 For these algorithms, 31 trials were run on each problem
328 instance in order to assess their average performance and
329 carry out statistical analyses.

330 All non-gradient algorithms are allowed 4096 func-
331 tion evaluations during the trials. Since absorption+ gra-
332 dient evaluations take approximately thrice the compu-
333 tational time (Eq. 11), SIMPf0 and SIMPf2 are allowed
334 1366 function evaluations.

335 The discrete algorithms, which only allow air or
336 porous elements in the design domain, are initiated from
337 random discrete solutions with equal probability of air
338 or porous material for each element (except for CH1 and
339 CH2). The continuous algorithms, which allow interme-
340 diate materials between air and porous materials in each
341 element, are initiated from solutions generated by assign-
342 ing a random number uniformly distributed between 0
343 and 1 to the topological design variables. Such random
344 initialisation is done to ensure a fair comparison making
345 no apriori assumptions about the solution.

346 Some of the newly proposed approaches, namely, hill
347 climbing, constructive heuristics, and the discrete vari-
348 ants of CMA evolution strategy and differential evolu-
349 tion, in the specific way used here are tested for the
350 first time in topology optimisation. The others are well-
351 established algorithms, and resources including surveys,
352 tutorials and code implementations can be easily reached.
353 More specific implementation details are included in the
354 supplementary material. It is noted that a thorough
355 knowledge of all the algorithms is not essential to under-
356 stand the findings. These algorithms can be thought of
357 as black-boxes that optimise the shape design by search-
358 ing for the optimal assignment of the decision variables
359 χ to maximise $\bar{\alpha}(\chi)$.

360 IV. RESULTS AND DISCUSSION

361 A. Run time performance comparison

362 One of the desired aspects of a good topology op-
363 timisation strategy is the ability to find better quality
364 solutions in a limited CPU time. As more CPU time is
365 allowed, the algorithms progressively find solutions with
366 higher absorption. Figure 2(a) compares the progress
367 of the best-so-far absorption values ($\bar{\alpha}$) obtained ver-
368 sus CPU time used by various algorithms on problem
369 instance 6.

370 Multiple machines were used to run the optimisation
371 tests, and in order to remove the machine-dependence
372 on runtime in Figure 2(a), the best-so-far absorption val-
373 ues were tracked against the number of function evalua-
374 tions, and runtimes were then computed by using aver-

375 age time-per-function-evaluation clocked on a reference
376 machine. The reference machine used features an In-
377 tel(R) Core(TM) i7-3820 CPU 3.6 GHz processor, 32
378 GB RAM and a 64-bit Windows 10 operating system
379 running Matlab2019b⁵⁵. Scales indicating the number of
380 function evaluations are also provided for benchmarking
381 purposes. For all non-deterministic algorithms, as mul-
382 tiple trials were conducted, the absorption values shown
383 in Figure 2(a) are averaged across the 31 trials after each
384 generation of the algorithm.

385 Firstly, note that initial absorption levels are differ-
386 ent for the algorithms. While the discrete algorithms
387 HC, GA, TABU, CMA_d and DE_d are initiated from ran-
388 dom discrete solutions with $\bar{\alpha}$ around 0.71, the continu-
389 ous algorithms CMA, DE, SIMPf0 and SIMPf2 are ini-
390 tiated from random continuous solutions with $\bar{\alpha}$ around
391 0.65. CH2 starts from fully porous design domain with
392 $\bar{\alpha}$ around 0.84 and CH1 starts from an empty (air-filled)
393 design domain with no absorption.

394 One of the first things to note is that the CH2 algo-
395 rithm does not produce an improvement from the fully
396 porous-filled solution and hence the best-so-far absorp-
397 tion value stays the same for this problem. For low CPU-
398 time budgets, SIMPf0 and SIMPf2 produce higher qual-
399 ity solutions than all the other algorithms except CH2.
400 SIMPf0 and SIMPf2 converge to a higher absorption than
401 the porous-filled CH2 solution in under 5 minutes on
402 this problem instance highlighting that gradient-based
403 methods can be time-efficient. After about 20 minutes of
404 runtime, HC produces better solutions on average than
405 SIMP, but the difference is small.

406 After the designated budget of 4096 function evalua-
407 tions (1366 gradient-included function evaluations), HC,
408 SIMPf2, TABU, SIMPf0 and CH1 produce the top tier
409 solutions. CMA_d follows closely by producing slightly
410 better-quality solutions compared to fully filled CH2 so-
411 lution towards the end. Whereas for DE_d and GA, the
412 runtime performance was considerably poor.

413 It is important to appreciate that the solutions from
414 continuous algorithms (CMA, DE, SIMPf0 and SIMPf2)
415 consider intermediate materials between the porous ma-
416 terial and air $\chi_i \in (0, 1]$ whereas the discrete algorithms
417 consider only porous material or air solutions $\chi_i \in \{0, 1\}$.
418 Since the solutions are from different search spaces, the
419 absorption levels cannot be directly compared between
420 the two. Although the final shapes from continuous algo-
421 rithms are desired to be 0 or 1, they are often not. Hence,
422 they are forced to be discrete using a simple round-off
423 filter, and the absorption values are recomputed. Such
424 rounding leads to a drop or surge in the absorption val-
425 ues at the end of all continuous algorithms as can be
426 observed noticeably in CMA and DE plotlines in Fig-
427 ure 2(a). The rounded absorptions indicated by the end
428 markers are also trial-averaged. Rounding leads to no
429 significant changes in SIMPf0 and SIMPf2 solutions for
430 this problem instance. For CMA and DE, the rounded
431 solution absorption values were poorer than SIMP solu-
432 tions.

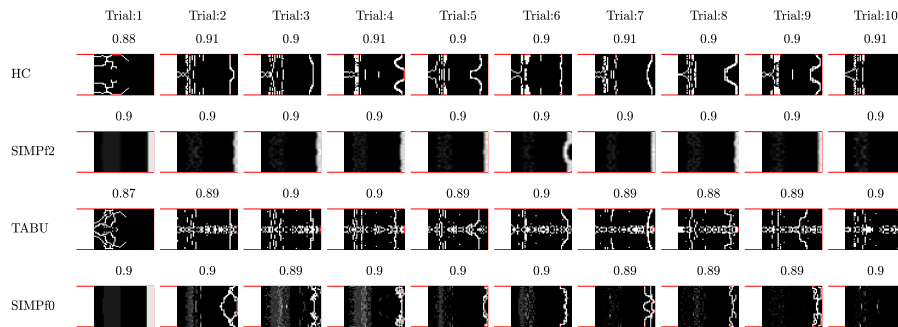
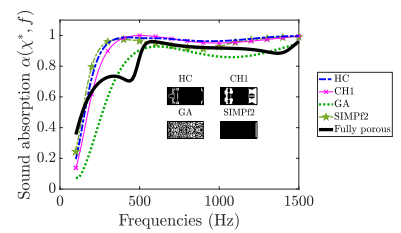
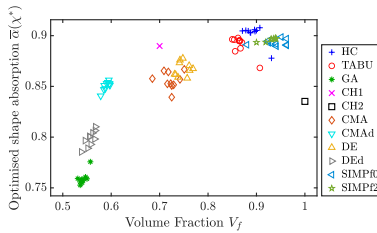
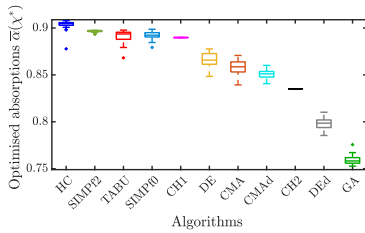
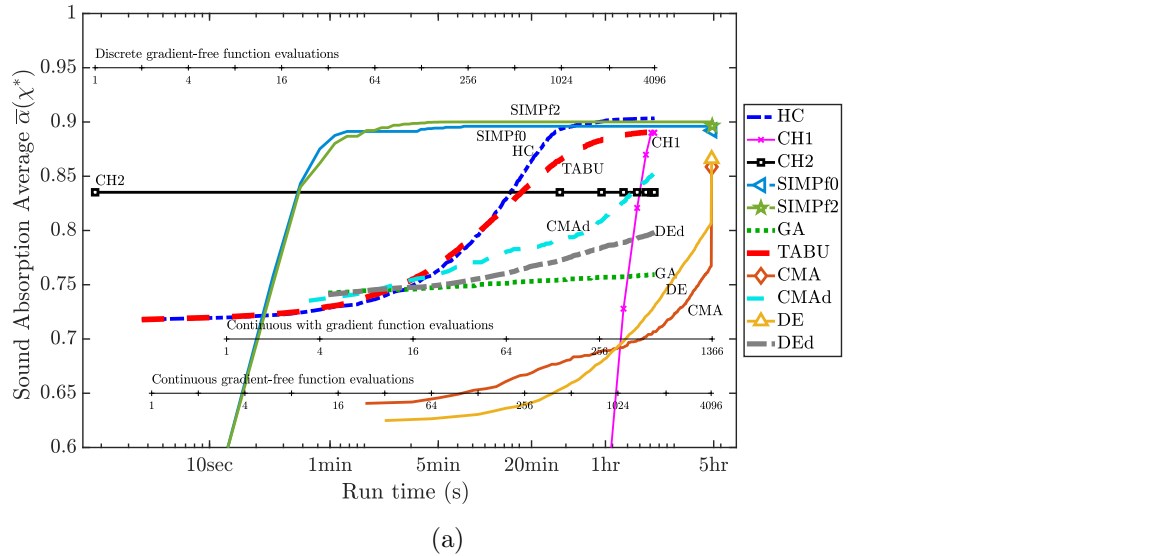


FIG. 2. (color online) Optimisation trials on problem instance 6: (a) Progress of best absorption found vs runtime (trial-averaged). For continuous algorithms, the solutions are discretised in the end. (b) Distribution of final solution absorption across trials. (c) Distribution of solution quality vs volume fraction (d) Sound absorption vs frequency for final shapes from select algorithms. (e) Best shapes from different trials from top four algorithms and their absorption.

433 The above behaviour of continuous algorithms does
 434 not seem to be the general trend across all problem
 435 instances. When considering the runtime performance of
 436 problem instance 1 shown in Figure 3, SIMP algorithms
 437 produce final solutions with intermediate materials which
 438 when rounded result in a significant reduction in absorp-

439 tion. This behaviour is also prominent in other problem
 440 instances especially the one with the high resistivity ma-
 441 terial (plots for other problem instances included in the
 442 supplementary material).

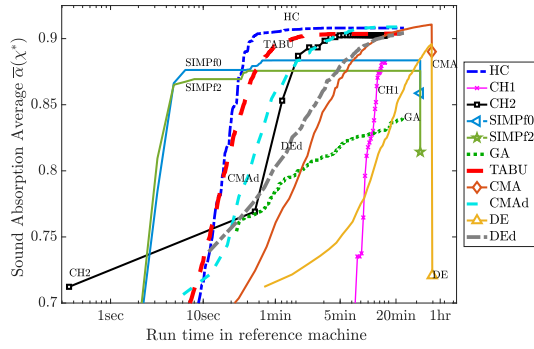


FIG. 3. (color online) Progress of best absorption found vs runtime: problem instance 1.

B. Final solution quality comparison

After rounding the continuous algorithm solutions and re-evaluating absorption, the distribution of final absorption values are shown in Figure 2(b). What is interesting to note is that for non-deterministic algorithms, the 31 trials do not necessarily result in the same optimised shapes and the final absorption values are spread out. The boxes enclose first to third quartiles (i.e. 25 percentile to 75 percentile), the whiskers denote the span, and the crosses denote the outliers.

Often in practice, a particular topology optimisation strategy may be chosen, and one trial may be run to determine a near-optimal shape. In such cases, it is desirable to pick an algorithm that has the best median performance across trials. Hence, using the median absorption across trials, the algorithms are sorted best to worst from left to right in Figure 2(b). HC and SIMPf2 turn out to be the top-performing algorithms for this problem instance followed by TABU, SIMPf0 and CH1 in the second tier. DE, CMA and CMAAd follow with all trials producing better solutions than the fully-filled CH2 solution. DEd and GA performed the poorest with no trials producing better than the fully-filled solution.

The shapes produced from 10 of the trials from the top four algorithms are displayed in Figure 2(e). Most shapes seem to have a thin layer of air near the rigid backing as this allows removing elastic resonance around 500 Hz as can be observed from the absorption curves in Figure 2(d). Without filtering, SIMPf0 produces intricate designs near this thin air layer compared to SIMPf2.

C. Performance across problem instances

For an overall comparison, the ranking is extended to other problem instances in Table IV. Such a comparison across many problem instances is essential as algorithms performing well on one problem instance need not necessarily perform well on other problem instances. The ranking scheme is such that if the median absorption values of two or more algorithms are the same correct to two decimal places, they are assigned the same rank.

TABLE IV. The algorithms are ranked based on median values of optimised shape absorption ($\bar{\alpha}^*$) across trials. Lesser the average rank, the better is the performance of the algorithm. Algorithms are sorted based on the average of the ranks across problem instances. This ranking scheme is provided for a quick lookup only and is not meant to be a precise indicator of the performance. The ranking could change if more problem instances and algorithms are considered.

Ranks	Problem instances \rightarrow Avg. rank						
Algorithms \downarrow	1	2	3	4	5	6	7
HC	1	1	3	1	1	1	1.29*
CMAAd	1	3	1	1	4	8	2.71
CH1	7	1	8	1	1	3	3.14
TABU	1	5	4	8	7	3	4.14
CH2	5	6	4	1	4	9	4.29
SIMPf0	8	3	10	1	4	3	5.43
SIMPf2	10	6	11	1	1	1	5.86
DEd	1	9	2	10	9	10	6
CMA	6	6	4	8	9	7	6.86
DE	11	11	9	1	7	6	7.71
GA	9	10	4	11	11	11	8.14

This ranking is only provided for a quick summary of the optimisation tests, and it is emphasised that the ranks may not be the same for a different set of problem instances.

From Table IV, one can observe that HC, CMAAd and CH1 rank among the top three. Although SIMPf2 and SIMPf0 performed well on problem instance 6, they take respectively the 6th and 7th places overall among the algorithms compared.

Surprisingly, the simple first-improvement hillclimbing (HC) ranks among the best in all problem instances except the high-resistivity material instance (problem instance 3). This means that HC's potential can be exploited by using it in hybrid algorithms. It is worth noting that HC applied to the MBB beam compliance minimisation⁶ results in the trivial fully-solid-filled solution. A simple way to avoid this is to use a volume fraction penalty with the objective function.

CMAAd and CH1 ranked first in four problem instances. Although CMAAd ranked 8th in problem instance 6, its overall performance across the problem instances puts the algorithm in second place. Notably, in problem instance 3, which considers a high static airflow resistivity material, CMAAd performed the best. This problem instance likely has many local optima and the performance of CMAAd indicates its global topology optimisation potential. The poor performance of the SIMP algorithms in this problem instance is likely due to the multi-modality of the objective function and premature convergence to local optima.

512 Although the progress of absorption in the initial
513 stages of CH1 is slow compared to the other algorithms,
514 the final absorption value makes CH1 one of the best
515 algorithms. Notably, for many problem instances con-
516 sidered, the best absorption value from CH1 is higher
517 than the absorption of the discretised solutions from both
518 SIMPf0 and SIMPf2. CH1 seems to be better overall
519 compared to CH2, indicating that constructing the solu-
520 tion from scratch may be better than removing material
521 from a fully-filled solution.

522 Performance of CMA and DE were relatively poor
523 in this benchmark. One reason could be that the num-
524 ber of design variables is large and these strategies do
525 not exploit the correlation of the neighbouring-element
526 design variables, a special attribute in topology optimi-
527 sation problems.

528 Both CMA_d and DE_d seem to perform better than
529 CMA and DE in general, indicating that rounding during
530 the algorithm may be a better approach than rounding
531 the solutions after the termination of continuous algo-
532 rithms. While CMA_d ranked among the top, the perfor-
533 mance of DE_d was similar to that of SIMP in terms of
534 solutions quality.

535 Among the algorithms considered, GA performed the
536 poorest. Though, scope for improvement exists in terms
537 of using better mutation and crossover operators adapted
538 to topology optimisation, focus may be diverted to other
539 strategies which show better promise.

540 D. Best shapes obtained from algorithms

541 The best solutions from all the algorithms for all
542 problem instances are plotted in Figure 4. For non-
543 deterministic algorithms, the solution with the highest
544 absorption among the 31 trials is shown. It is recalled
545 that manufacturability restrictions and morphological fil-
546 ters are not imposed in this study except for SIMPf2.
547 Results show both SIMPf0 and SIMPf2 produce similar
548 shapes for most problem instances.

549 For problem instance 1, all algorithms except SIMPf2
550 result in irregular shapes. The best quality shapes from
551 most algorithms are flat layers of air and porous material
552 towards the rigid wall with a somewhat circular air cavity
553 in the front. GA and DE produced checkerboard shapes.
554 Moreover, shapes from GA for all problem instances are
555 degenerate.

556 For problem instance 2, HC, CH1 and SIMPf0 pro-
557 duce the best shape with an almost porous material filled
558 design domain except for a layer of air next to the rigid
559 wall. CH1, SIMPf2, CMA, CMA_d, TABU produced sim-
560 ilar shapes. CH2 resulted in a fully-filled shape with
561 slightly less absorption.

562 In problem instance 3 with a high static airflow res-
563 sistivity material, the shapes from all algorithms were
564 seemingly random patterns but with sort of a cavity in
565 the centre. SIMPf2 produces a result with a chunk of
566 porous material suspended in the air.

567 For problem instance 4, the optimal solution seems
568 to be a fully-filled design domain and most algorithms

569 are able to find this except for GA. The reason could be
570 that GA is initiated from random bit arrays which would
571 have volume fraction distributed near 50 percent (central
572 limit theorem). Thus, initialising GA with solutions with
573 a range of volume fractions might be a sounder approach.

574 For problem instance 5, many algorithms find a solu-
575 tion with a shape almost filled with the porous material
576 except for air pockets near the rigid wall. CMA, DE and
577 DE_d seem to be approaching this solution. CH2 com-
578 pletely fills the design domain with the porous material.

579 For problem instance 6, the fully-filled solution has
580 an elastic resonance in the frequency range considered,
581 as may be seen from Figure 2(d). The elastic resonance
582 forms a drop in the absorption near 500 Hz. The best so-
583 lutions from different algorithms effectively remove this
584 resonance. To do this, the algorithms seem to introduce
585 air layers at the front and near the rigid backing. CMA,
586 CMA_d, DE and DE_d give checker-board shapes which
587 somewhat removes a layer near the rigid backing. No-
588 tably, CH1 gives a smooth shape even though no man-
589 ufacturability restrictions were imposed. CH2 returns a
590 filled design domain and is unable to get rid of the reso-
591 nance.

592 For problem instance 7, many solutions have close
593 to complete sound absorption ($\bar{\alpha} = 1$). Almost all al-
594 gorithms find solutions with total sound absorption at
595 500 Hz. Notably, SIMPf0 and SIMPf2 seem to suggest a
596 fully-filled solution.

597 In general, the algorithms which feature random
598 move operations tend to produce degenerate shapes. Al-
599 though hill climbing results in shapes with high sound
600 absorption, the shapes obtained are sometimes irregu-
601 lar and need additional filtering. On the other hand,
602 constructive heuristic with material addition (CH1) has
603 both high performance and finds shapes with smoother
604 boundaries.

605 In summary, different algorithms seem to provide so-
606 lutions from a unique pool (Figure 2(c)). The reason
607 for this is each approach uses unique move operations
608 during the optimisation to reach solutions that may not
609 be explored by other algorithms. Thus it may be worth
610 many optimisation strategies to find a set of unique solu-
611 tions which may be of interest to the acoustic engineer.
612 In addition, scope for improving many of these methods
613 exist. As an example, the performance of SIMP could
614 be improved by using better strategies for avoiding lo-
615 cal optima, and an appropriate morphological filter may
616 be used in CMA_d to overcome the drawback of produc-
617 ing unconnected shapes while speeding up the algorithm.
618 The results outlined in this article provides an initial un-
619 derstanding of various heuristics and metaheuristics per-
620 form on topology optimisation for absorption maximisa-
621 tion. Thus, guidelines for developing hybrid algorithms
622 and hyper-heuristics may be arrived at for devising more
623 time-efficient strategies that also produce solutions closer
624 to the true optima.

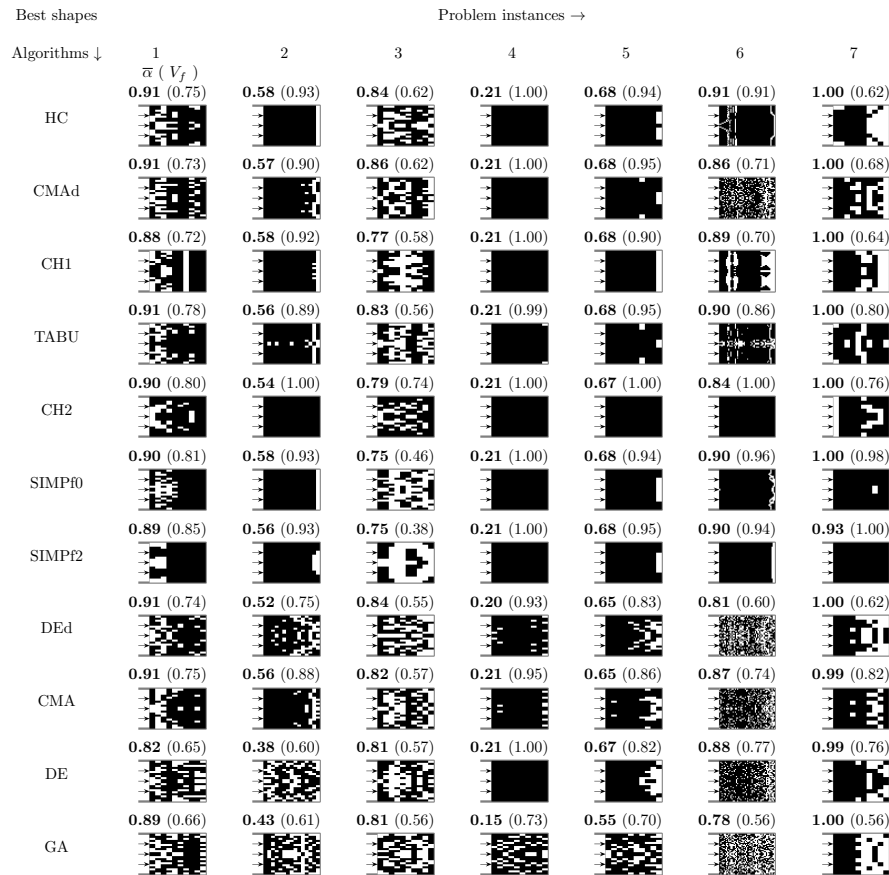


FIG. 4. Optimised shapes obtained from all algorithms for each problem instance. The shapes are discretised by rounding for continuous algorithms. The values of mean absorption across frequencies ($\bar{\alpha}$) are printed at the top of each shape in bold font along with porous material volume fraction (V_f) in parentheses. White and black represent air and the porous, respectively, with the acoustic input on the left and rigid backing on the right.

625 V. CONCLUSIONS

626 In this work, topology optimisation to max-
 627 imise sound absorption under normal incidence in an
 628 impedance tube with a rigid backing is considered.
 629 Optimisation tests were conducted using 5 heuristic
 630 and 6 metaheuristic algorithms on 7 benchmark prob-
 631 lem instances. The approaches include hill climb-
 632 ing (HC), constructive heuristics (CH1 and CH2),
 633 solid-isotropic-material-with-penalisation (SIMPf0 and
 634 SIMPf2), genetic algorithm (GA), tabu search (TABU),
 635 covariance-matrix-adaptation evolution strategy (CMA
 636 and CMAAd), and differential evolution (DE and DED).
 637 Unlike in usual structural topology optimisation prob-
 638 lems, volume fraction constraint and manufacturability
 639 filters were not imposed. The highlights of the findings
 640 are as follows.

- 641 • Gradient algorithms (SIMPf0 and SIMPf2) can
 642 quickly converge to good quality solutions, but in

643 some problems, they either prematurely converge
 644 to local optima or produce shapes that have in-
 645 termediate materials indicating that the objective
 646 function is multimodal with many local optima.

- 647 • When comparing the solution quality, no algo-
 648 rithm clearly outperformed all others on all of
 649 the problem instances. Ranking the algorithms
 650 based on median solution quality revealed that
 651 the hill climbing approach performed the best, fol-
 652 lowed by the material-addition constructive heuris-
 653 tic (CH1), and the discrete variant of covariance-
 654 matrix-adaptation evolution strategy (CMAAd).
- 655 • The optimal shapes produced by algorithms that
 656 use stochastic components (GA, CMA, CMAAd, DE,
 657 DED) tend to be irregular and unconnected, and
 658 hence they might need additional filtering tech-
 659 niques. Although HC produced higher sound ab-
 660 sorption solutions in general, the optimal shapes

661 produced were not smooth and crisp. On the other
 662 hand, CH1 produces high-quality solutions that
 663 also have fewer irregularities than HC. In addition
 664 to this, the sound absorption values of shapes pro-
 665 duced by CH1 were as good as or slightly better
 666 than those produced by SIMP ρ_0 . Moreover, CH1
 667 can be easily modified to include volume fraction
 668 constraint by terminating the construction after the
 669 desired volume fraction is reached. The material
 670 removal heuristic (CH2) often returns a fully filled
 671 design domain as the solution, and the reason for
 672 this is not clear.

- 673 • Between the continuous algorithms (CMA and DE)
 674 and their discrete variants (CMAd and DEd), the
 675 discrete variants seem to perform better. This
 676 means using filtering techniques before each objec-
 677 tive function evaluation works better than filtering
 678 the solutions at the end of the algorithm.

679 To conclude, the absorption maximisation topology
 680 optimisation problem seems to be rich with many local-
 681 optimal solutions, and different strategies explore differ-
 682 ent regions of the search space producing unique varieties
 683 of solutions. Insights obtained may be valuable in de-
 684 signing hybrid strategies and hyperheuristics for general-
 685 purpose optimisation of sound-absorbing materials.

686 ACKNOWLEDGEMENT

687 The authors thank the anonymous reviewers whose
 688 suggestions have greatly improved the manuscript. This
 689 work is part of a project that has received funding from
 690 the European Research Council (ERC) under the Euro-
 691 pean Union’s Horizon 2020 research and innovation pro-
 692 gramme *No2Noise* (Grant agreement No. 765472).

693 ¹Martin P Bendsøe and N Kikuchi. Generating optimal topolo-
 694 gies in structural design using a homogenization method. *Comp.*
 695 *Meth. App. Mech. Eng.*, 71(2):197–224, 1988.

696 ²Mathias Stolpe and Martin P Bendsøe. Global optima for the
 697 Zhou–Rozvany problem. *Struct. Multi. Optim.*, 43(2):151–164,
 698 2011.

699 ³M Zhou and GIN Rozvany. On the validity of ESO type methods
 700 in topology optimization. *Struct. Multi. Optim.*, 21(1):80–83,
 701 2001.

702 ⁴Martin P Bendsøe. Optimal shape design as a material distribu-
 703 tion problem. *Struct. Optim.*, 1(4):193–202, 1989.

704 ⁵M Zhou and GIN Rozvany. The coc algorithm, part ii: Topo-
 705 logical, geometrical and generalized shape optimization. *Comp.*
 706 *Meth. App. Mech. Eng.*, 89(1-3):309–336, 1991.

707 ⁶Ole Sigmund. A 99 line topology optimization code written in
 708 Matlab. *Struct. Multi. Optim.*, 21(2):120–127, 2001.

709 ⁷Yi M Xie and Grant P Steven. A simple evolutionary procedure
 710 for structural optimization. *Comp. & Struct.*, 49(5):885–896,
 711 1993.

712 ⁸YM Xie and GP Steven. Evolutionary structural optimization
 713 for dynamic problems. *Comp. & Struct.*, 58(6):1067–1073, 1996.

714 ⁹XY Yang, YM Xie, GP Steven, and OM Querin. Topology opti-
 715 mization for frequencies using an evolutionary method. *J. Struct.*
 716 *Eng.*, 125(12):1432–1438, 1999.

717 ¹⁰Michael Yu Wang, Xiaoming Wang, and Dongming Guo. A level
 718 set method for structural topology optimization. *Comp. Meth.*
 719 *App. Mech. Eng.*, 192(1-2):227–246, 2003.

720 ¹¹Grégoire Allaire, François Jouve, and Anca-Maria Toader. Struc-
 721 tural optimization using sensitivity analysis and a level-set
 722 method. *J. Comp. Physics*, 194(1):363–393, 2004.

723 ¹²Martin Burger, Benjamin Hackl, and Wolfgang Ring. Incorpor-
 724 ating topological derivatives into level set methods. *J. Comp.*
 725 *Physics*, 194(1):344–362, 2004.

726 ¹³Martin P Bendsøe and Ole Sigmund. *Optimization of structural*
 727 *topology, shape, and material*, volume 414. Springer, 1995.

728 ¹⁴Krister Svanberg. The method of moving asymptotes—a new
 729 method for structural optimization. *Int. J. Num. Meth. Eng.*,
 730 24(2):359–373, 1987.

731 ¹⁵Fred Glover and Manuel Laguna. Tabu search. In *Handbook of*
 732 *comb. optim.*, pages 2093–2229. Springer, 1998.

733 ¹⁶David Guirguis, Nikola Aulig, Renato Picelli, Bo Zhu, Yuqing
 734 Zhou, William Vicente, Francesco Iorio, Markus Olhofer, Woj-
 735 ciech Matusik, Carlos Artemio Coello Coello, et al. Evolution-
 736 ary black-box topology optimization: Challenges and promises.
 737 *IEEE Trans. Evol. Comp.*, 2019.

738 ¹⁷Pooya Rostami and Javad Marzbanrad. Identification of opti-
 739 mal topologies for continuum structures using metaheuristics: A
 740 comparative study. *Arch. Comp. Meth. Eng.*, pages 1–28, 2021.

741 ¹⁸Martin Philip Bendsøe and Ole Sigmund. *Topology optimization:*
 742 *theory, methods, and applications*. Springer Sci. & Bus. Media,
 743 2013.

744 ¹⁹Ole Sigmund and Kurt Maute. Topology optimization ap-
 745 proaches. *Struct. Multi. Optim.*, 48(6):1031–1055, 2013.

746 ²⁰GIN Rozvany. Aims, scope, methods, history and unified ter-
 747 minology of computer-aided topology optimization in structural
 748 mechanics. *Struct. Multi. Optim.*, 21(2):90–108, 2001.

749 ²¹Joshua D Deaton and Ramana V Grandhi. A survey of structural
 750 and multidisciplinary continuum topology optimization: post
 751 2000. *Struct. Multi. Optim.*, 49(1):1–38, 2014.

752 ²²Eddie Wadbro and Martin Berggren. Topology optimization of
 753 an acoustic horn. *Comp. meth. app. mech. eng.*, 196(1-3):420–
 754 436, 2006.

755 ²³Maria B Dühring, Jakob S Jensen, and Ole Sigmund. Acoustic
 756 design by topology optimization. *J. Sound Vib.*, 317(3-5):557–
 757 575, 2008.

758 ²⁴Joong Seok Lee, Yoon Young Kim, Jung Soo Kim, and Yeon June
 759 Kang. Two-dimensional poroelastic acoustical foam shape design
 760 for absorption coefficient maximization by topology optimization
 761 method. *J. Acous. Soc. America*, 123(4):2094–2106, 2008.

762 ²⁵Jin Woo Lee and Yoon Young Kim. Topology optimization of
 763 muffler internal partitions for improving acoustical attenuation
 764 performance. *Int. J. Num. Meth. Eng.*, 80(4):455–477, 2009.

765 ²⁶Junghwan Kook, Kunmo Koo, Jaeyub Hyun, Jakob S Jensen,
 766 and Semyung Wang. Acoustical topology optimization for
 767 Zwicker’s loudness model-application to noise barriers. *Comp.*
 768 *Meth. App. Mech. Eng.*, 237:130–151, 2012.

769 ²⁷Gil Ho Yoon. Acoustic topology optimization of fibrous material
 770 with Delany–Bazley empirical material formulation. *J. Sound*
 771 *Vib.*, 332(5):1172–1187, 2013.

772 ²⁸Joong Seok Lee, Peter Göransson, and Yoon Young Kim. Topol-
 773 ogy optimization for three-phase materials distribution in a dis-
 774 sipative expansion chamber by unified multiphase modeling ap-
 775 proach. *Comp. Meth. App. Mech. Eng.*, 287:191–211, 2015.

776 ²⁹Ki Hyun Kim and Gil Ho Yoon. Optimal rigid and porous mate-
 777 rial distributions for noise barrier by acoustic topology optimiza-
 778 tion. *J. Sound Vib.*, 339:123–142, 2015.

779 ³⁰Esubalewe Lakie Yedeg, Eddie Wadbro, and Martin Berggren. In-
 780 terior layout topology optimization of a reactive muffler. *Struct.*
 781 *Multi. Optim.*, 53(4):645–656, 2016.

782 ³¹Leilei Chen, Cheng Liu, Wenchang Zhao, and Linchao Liu. An
 783 isogeometric approach of two dimensional acoustic design sensi-
 784 tivity analysis and topology optimization analysis for absorbing
 785 material distribution. *Comp. Meth. App. Mech. Eng.*, 336:507–
 786 532, 2018.

- 787 ³²Junghwan Kook. Evolutionary topology optimization for
788 acoustic-structure interaction problems using a mixed u/p for-
789 mulation. *Mech. Based Des. Struct. and Mach.*, 47(3):356–374,
790 2019.
- 791 ³³Won Uk Yoon, Jun Hyeong Park, Joong Seok Lee, and
792 Yoon Young Kim. Topology optimization design for total sound
793 absorption in porous media. *Comp. Meth. App. Mech. Eng.*,
794 360:112723, 2020.
- 795 ³⁴Yanming Xu, Wenchang Zhao, Leilei Chen, and Haibo Chen.
796 Distribution optimization for acoustic design of porous layer by
797 the boundary element method. *Acous. Australia*, pages 1–13,
798 2020.
- 799 ³⁵Leilei Chen, Chuang Lu, Haojie Lian, Zhaowei Liu, Wenchang
800 Zhao, Shengze Li, Haibo Chen, and Stéphane PA Bordas. Acous-
801 tic topology optimization of sound absorbing materials directly
802 from subdivision surfaces with isogeometric boundary element
803 methods. *Comp. Meth. App. Mech. Eng.*, 362:112806, 2020.
- 804 ³⁶Zi-xiang Xu, Hao Gao, Yu-jiang Ding, Jing Yang, Bin Liang, and
805 Jian-chun Cheng. Topology-optimized omnidirectional broad-
806 band acoustic ventilation barrier. *Phy. Rev. App.*, 14(5):054016,
807 2020.
- 808 ³⁷Ole Sigmund and Peter Michael Clausen. Topology optimization
809 using a mixed formulation: an alternative way to solve pressure
810 load problems. *Comp. Meth. App. Mech. Eng.*, 196(13-16):1874–
811 1889, 2007.
- 812 ³⁸Gil Ho Yoon, Jakob Søndergaard Jensen, and Ole Sigmund.
813 Topology optimization of acoustic-structure interaction prob-
814 lems using a mixed finite element formulation. *Int. J. Num.*
815 *Meth. Eng.*, 70(9):1049–1075, 2007.
- 816 ³⁹Peter Göransson, Jacques Cuenca, and Timo Lähivaara. Param-
817 eter estimation in modelling frequency response of coupled sys-
818 tems using a stepwise approach. *Mech. Sys. Sig. Proc.*, 126:161–
819 175, 2019.
- 820 ⁴⁰Krister Svanberg. A class of globally convergent optimization
821 methods based on conservative convex separable approximations.
822 *SIAM J. Optim.*, 12(2):555–573, 2002.
- 823 ⁴¹Noureddine Atalla, Raymond Panneton, and Patricia Debergue.
824 A mixed displacement-pressure formulation for poroelastic mat-
825 erials. *J. Acous. Soc. America*, 104(3):1444–1452, 1998.
- 826 ⁴²Francois-Xavier Bécot and Luc Jaouen. An alternative Biot’s for-
827 mulation for dissipative porous media with skeleton deformation.
828 *J. Acous. Soc. America*, 134(6):4801–4807, 2013.
- 829 ⁴³Hiroshi Isakari, Kohei Kuriyama, Shinya Harada, Takayuki Ya-
830 mada, Toru Takahashi, and Toshiro Matsumoto. A topology
831 optimisation for three-dimensional acoustics with the level set
832 method and the fast multipole boundary element method. *Mech.*
833 *Eng. J.*, 1(4):CM0039–CM0039, 2014.
- 834 ⁴⁴Vivek T. Ramamoorthy, Ender Özcan, Andrew J. Parkes, Abhi-
835 lash Sreekumar, Luc Jaouen, and François-Xavier Bécot. Acous-
836 tic topology optimisation using CMA-ES. In *Proceedings of*
837 *ISMA 2020 and USD 2020*, pages 511–522, 2020.
- 838 ⁴⁵David Linton Johnson, Joel Koplik, and Roger Dashen. Theory
839 of dynamic permeability and tortuosity in fluid-saturated porous
840 media. *J. Fluid Mech.*, 176:379–402, 1987.
- 841 ⁴⁶Yvan Champoux and Jean-F Allard. Dynamic tortuosity and
842 bulk modulus in air-saturated porous media. *J. App. Physics*,
843 70(4):1975–1979, 1991.
- 844 ⁴⁷Denis Lafarge, Pavel Lemarinier, Jean F Allard, and Viggo
845 Tarnow. Dynamic compressibility of air in porous structures at
846 audible frequencies. *J. Acous. Soc. America*, 102(4):1995–2006,
847 1997.
- 848 ⁴⁸Martin P Bendsøe and Ole Sigmund. Material interpolation
849 schemes in topology optimization. *Arch. App. Mech.*, 69(9-
850 10):635–654, 1999.
- 851 ⁴⁹Erik Andreassen, Anders Clausen, Mattias Schevenels, Boyan S
852 Lazarov, and Ole Sigmund. Efficient topology optimization in
853 MATLAB using 88 lines of code. *Struct. Multi. Optim.*, 43(1):1–
854 16, 2011.
- 855 ⁵⁰John Henry Holland et al. *Adaptation in natural and artificial*
856 *systems: an introductory analysis with applications to biology,*
857 *control, and artificial intelligence.* MIT press, 1992.
- 858 ⁵¹Fred Glover. Future paths for integer programming and links
859 to artificial intelligence. *Comp. & op. research*, 13(5):533–549,
860 1986.
- 861 ⁵²Nikolaus Hansen. The CMA evolution strategy: A tutorial. *arXiv*
862 *preprint arXiv:1604.00772*, 2016.
- 863 ⁵³Rainer Storn. On the usage of differential evolution for function
864 optimization. In *Proc. North American Fuzzy Inf. Proc.*, pages
865 519–523. IEEE, 1996.
- 866 ⁵⁴Rainer Storn and Kenneth Price. Differential evolution—a sim-
867 ple and efficient heuristic for global optimization over continuous
868 spaces. *J. Global Optim.*, 11(4):341–359, 1997.
- 869 ⁵⁵MATLAB. *version 9.7.0.1216025 (R2019b) Update 1.* The
870 MathWorks Inc., Natick, Massachusetts, 2019.

